SUPPORTING INFORMATION

Facile conversion of waste glass into Li storage materials

Seung-Su Lee[a] *and Cheol-Min Park*[a*]

[a]School of Materials Science and Engineering, Kumoh National Institute of Technology, Gumi, Gyeongbuk 39177, Republic of Korea

[*]Cheol-Min Park. Tel.: +82-54-478-7746; Fax: +82-54-478-7769

E-mail: cmpark@kumoh.ac.kr

Figure S1.

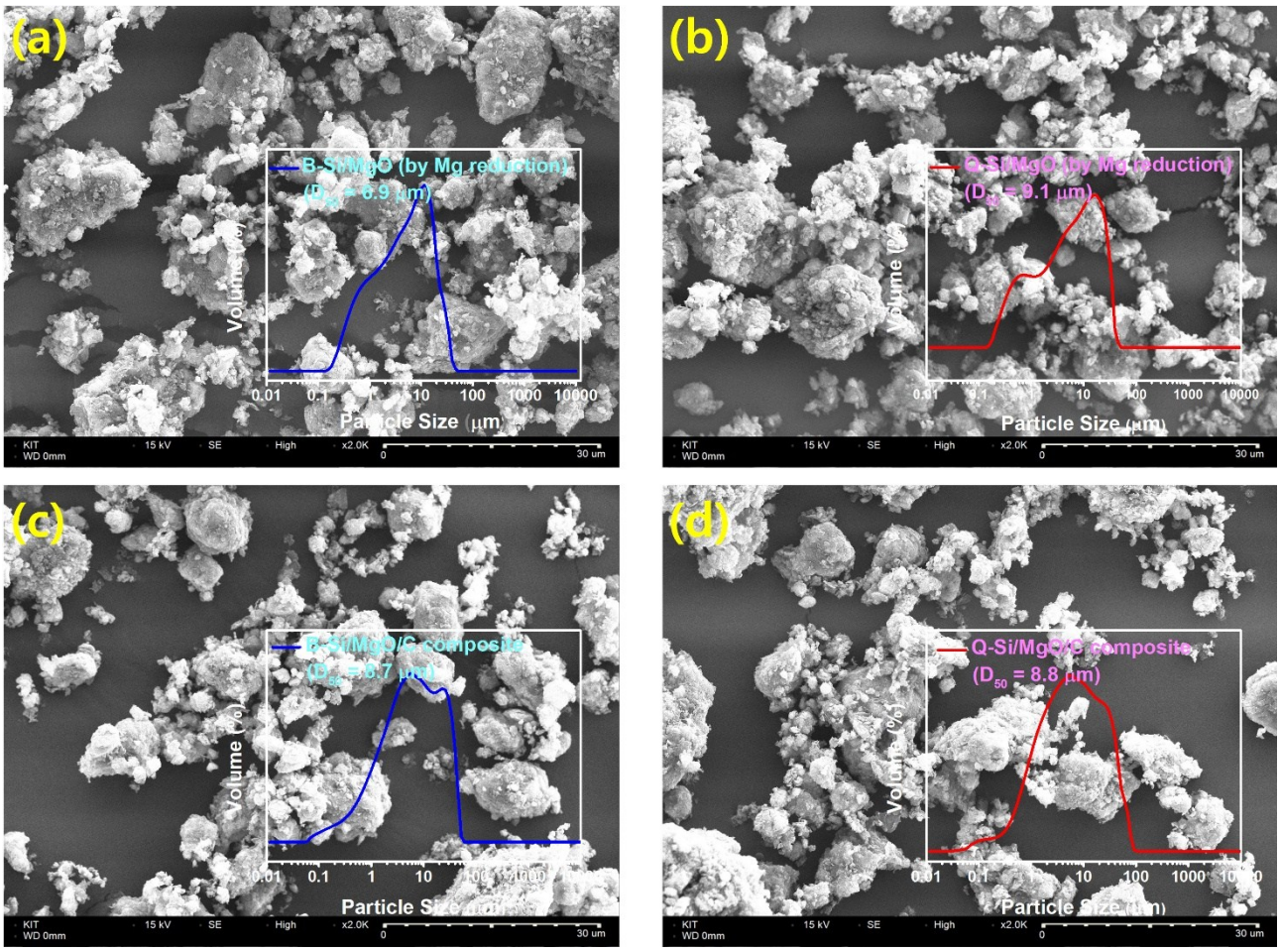

Figure S1. Particle size and morphology of Si/MgO and Si/MgO/C. SEM images and particle size distributions of (a) B-Si/MgO, (b) Q-Si/MgO, (c) B-Si/MgO/C, and (d) Q-Si/MgO/C.

Figure S2.

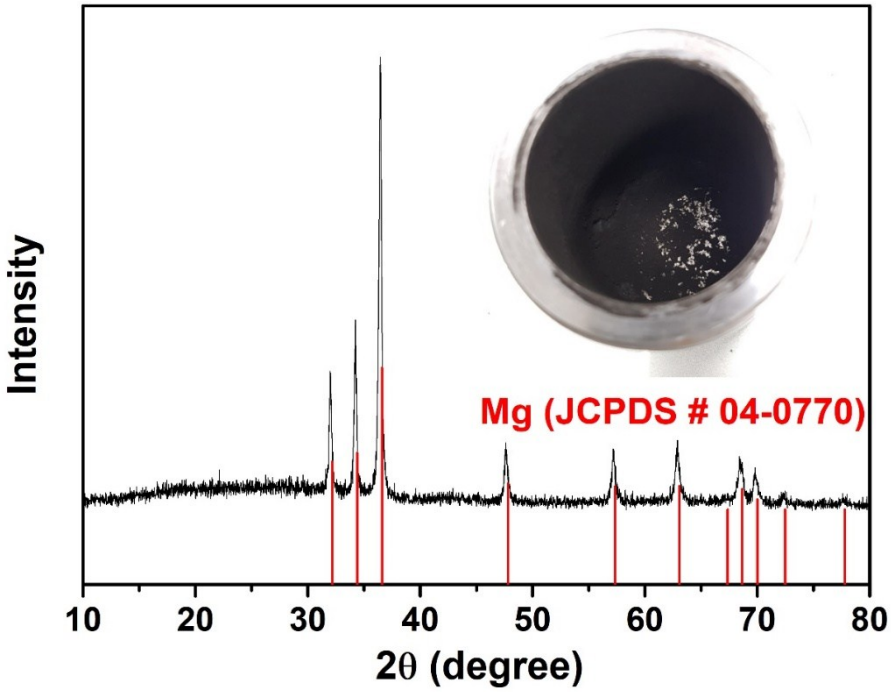

Figure S2. XRD and photography of S-Si/MgO. The S-Si/MgO was formed by the high-energy BM process using soda-lime glass and Mg powders.

Figure S3

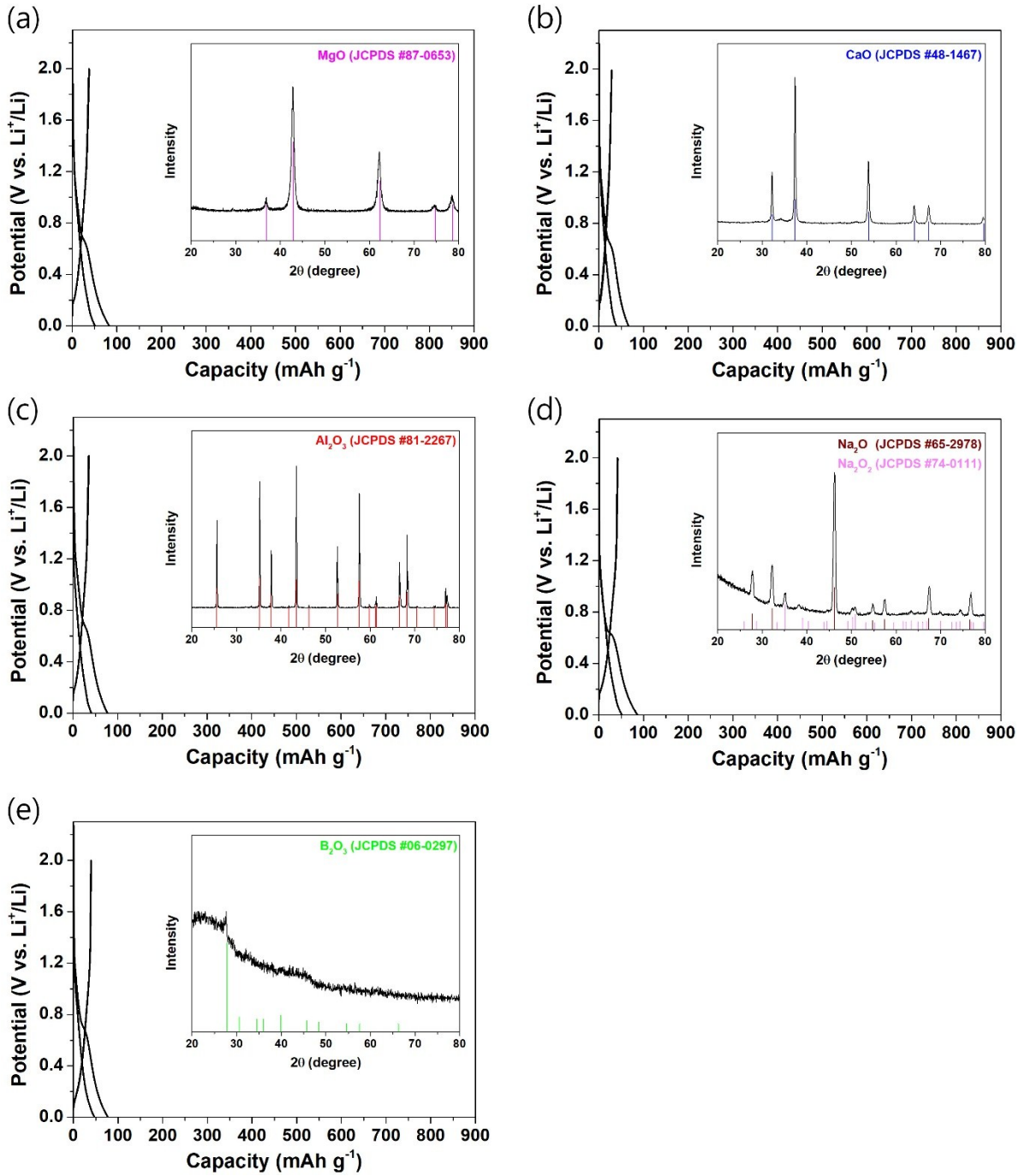

Figure S3. Electrochemical performances of various glass forming oxides. Voltage profiles and XRD results of (a) MgO, (b) CaO, (c) Al_2O_3, (d) Na_2O, and (e) B_2O_3.

Figure S4

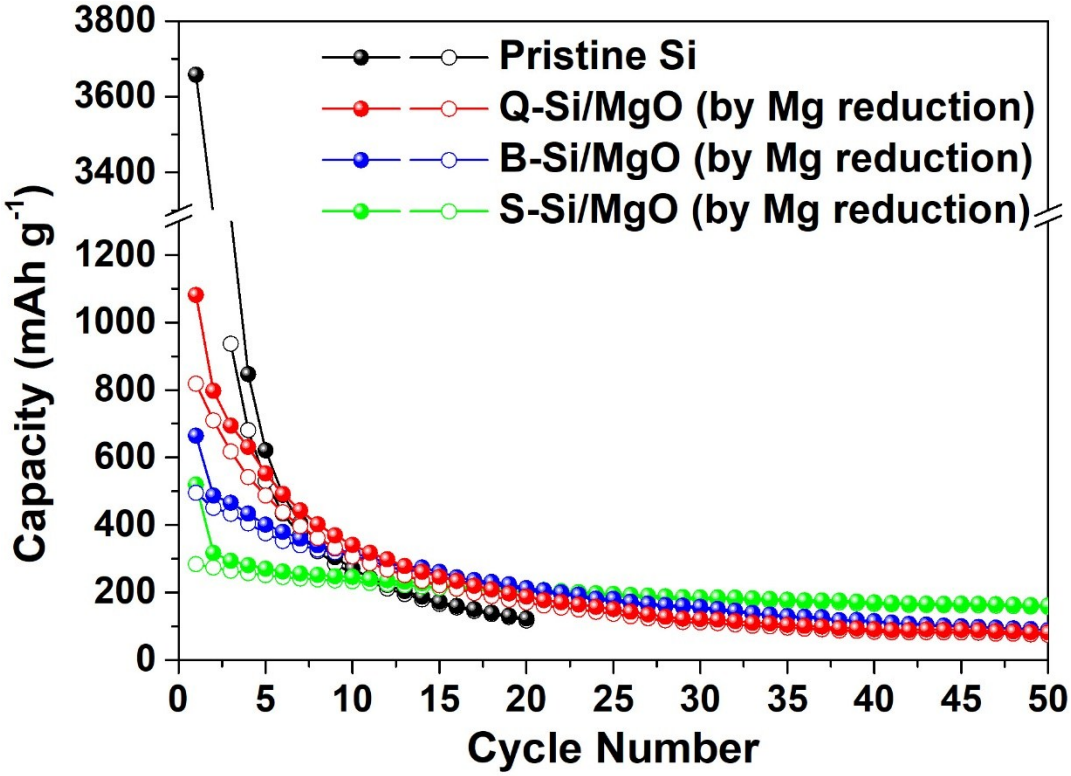

Figure S4. Cycling performance results for Si, Q-Si/MgO, B-Si/MgO, and S-Si/MgO electrodes.

Figure S5.

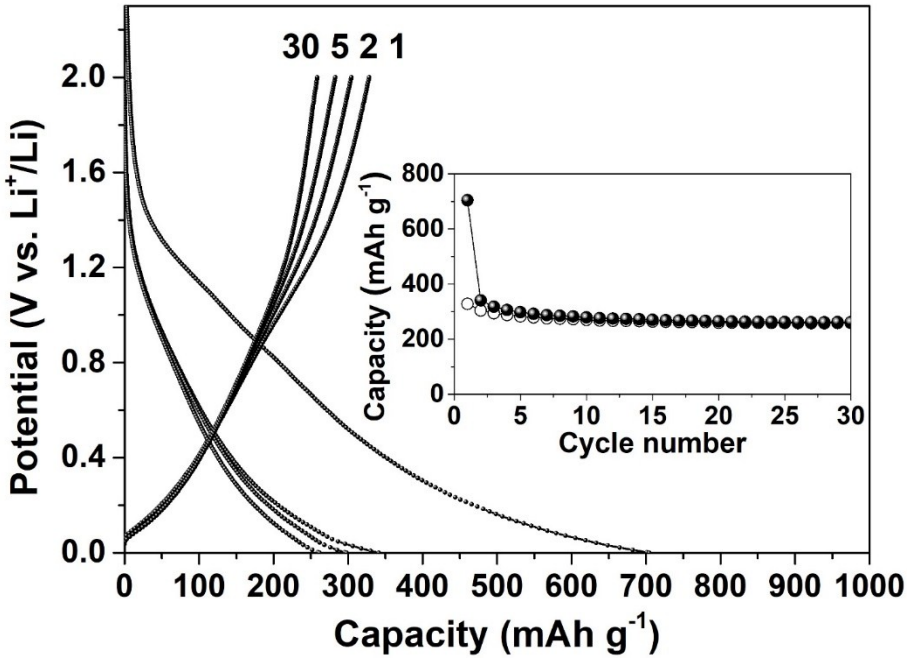

Figure S5. Electrochemical performances of the ball-milled C (Super P) electrode. Voltage profile of the ball-milled C at a current density of 100 mA g^{-1} (Inset: Cycling behavior of the ball-milled C at a cycling rate of 100 mA g^{-1}).

Figure S6.

Electrodes	Electrodes before Li-reaction	Li-inserted (0 V)	Li-extracted (2 V)
(a) Si	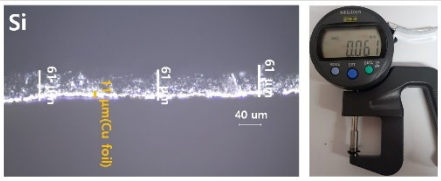 61 - 11 (Cu foil) = 50 μm (active material)	 126 – 11 (Cu) = 115 μm [**130.0%**]	 80 – 11 (Cu) = 69 μm [**38.0%**]
(b) Si/C composite	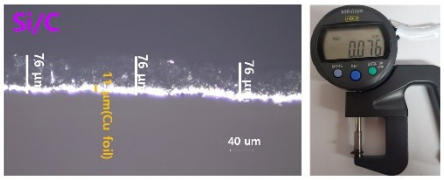 76 - 11 (Cu foil) = 65 μm (active material)	 116 – 11 (Cu) = 105 μm [**61.5%**]	 86 – 11 (Cu) = 75 μm [**15.4%**]
(c) B-Si/MgO/C composite	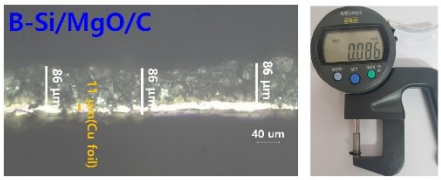 86 - 11 (Cu foil) = 75 μm (active material)	 108 – 11 (Cu) = 97 μm [**29.3%**]	 90 – 11 (Cu) = 79 μm [**5.3%**]
(d) Q-Si/MgO/C composite	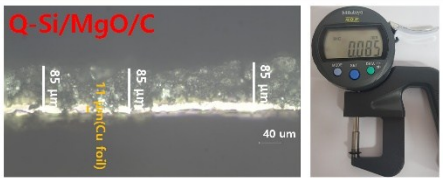 85 - 11 (Cu foil) = 74 μm (active material)	 112 – 11 (Cu) = 101 μm [**36.5%**]	 92 – 11 (Cu) = 81 μm [**9.5%**]

Figure S6. Electrode thickness changes in Si, Si/C, B-Si/MgO/C, and Q-Si/MgO/C electrodes according to the state-of-charge. (a) Swelling data of Si electrode (before Li-reaction, Li-inserted at 0 V, and Li-extracted at 2 V). (b) Swelling data of Si/C composite electrode (before Li-reaction, Li-inserted at 0 V, and Li-extracted at 2 V). (c) Swelling data of B-Si/MgO/C composite electrode (before Li-reaction, Li-inserted at 0 V, and Li-extracted at 2 V). (d) Swelling data of Q-Si/MgO/C composite electrode (before Li-reaction, Li-inserted at 0 V, and Li-extracted at 2 V).

Figure S7.

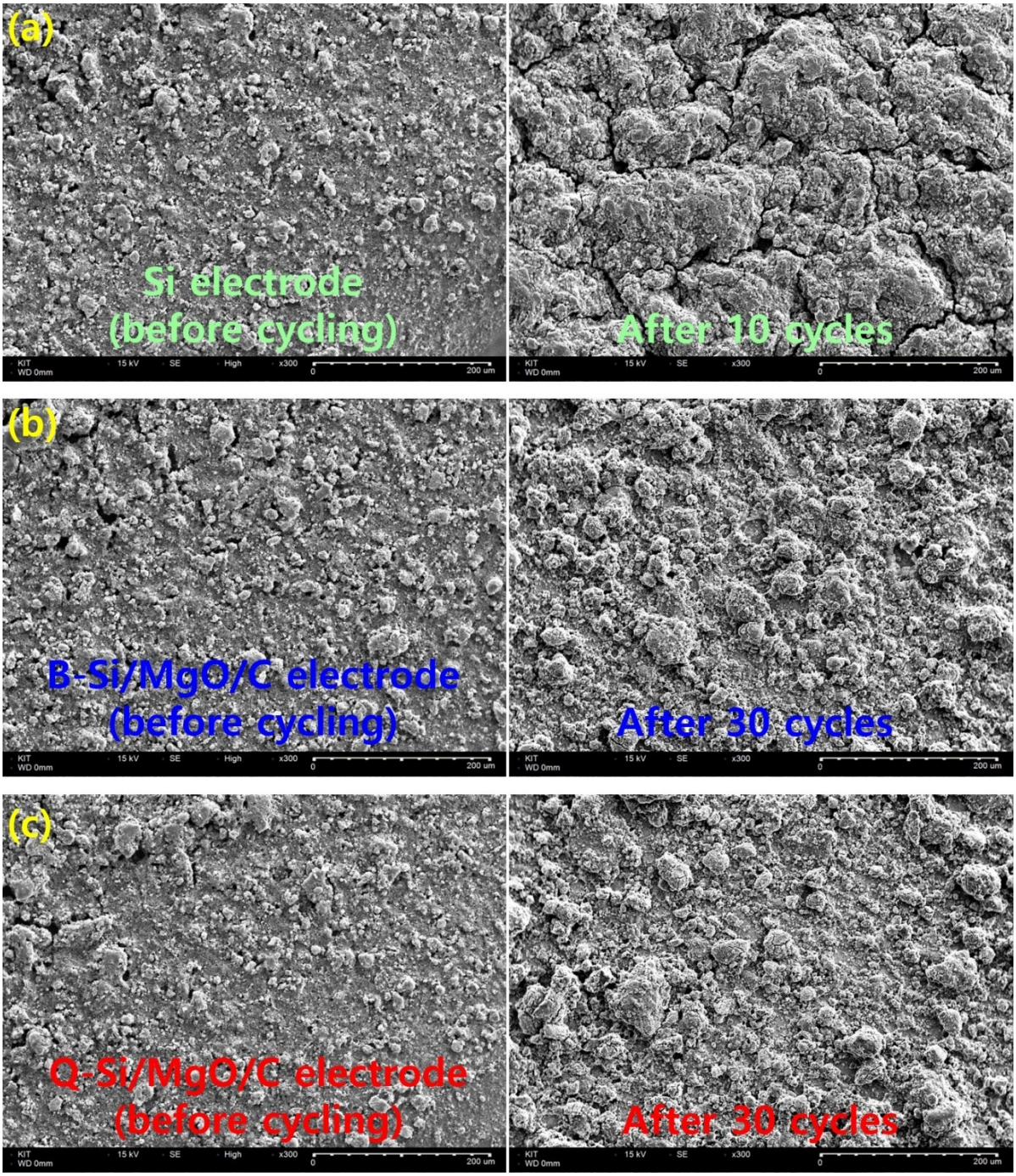

Figure S7. Morphological investigation using *ex-situ* SEM of the Si, B-Si/MgO/C, and Q-Si/MgO/C electrodes during cycling. (a) *Ex-situ* SEM results of the pristine Si electrode before cycling and after 10 cycles. (b) *Ex-situ* SEM results of the B-Si/MgO/C electrode before cycling and after 30 cycles. (c) *Ex-situ* SEM results of the Q-Si/MgO/C electrode before cycling and after 30 cycles.

Figure S8.

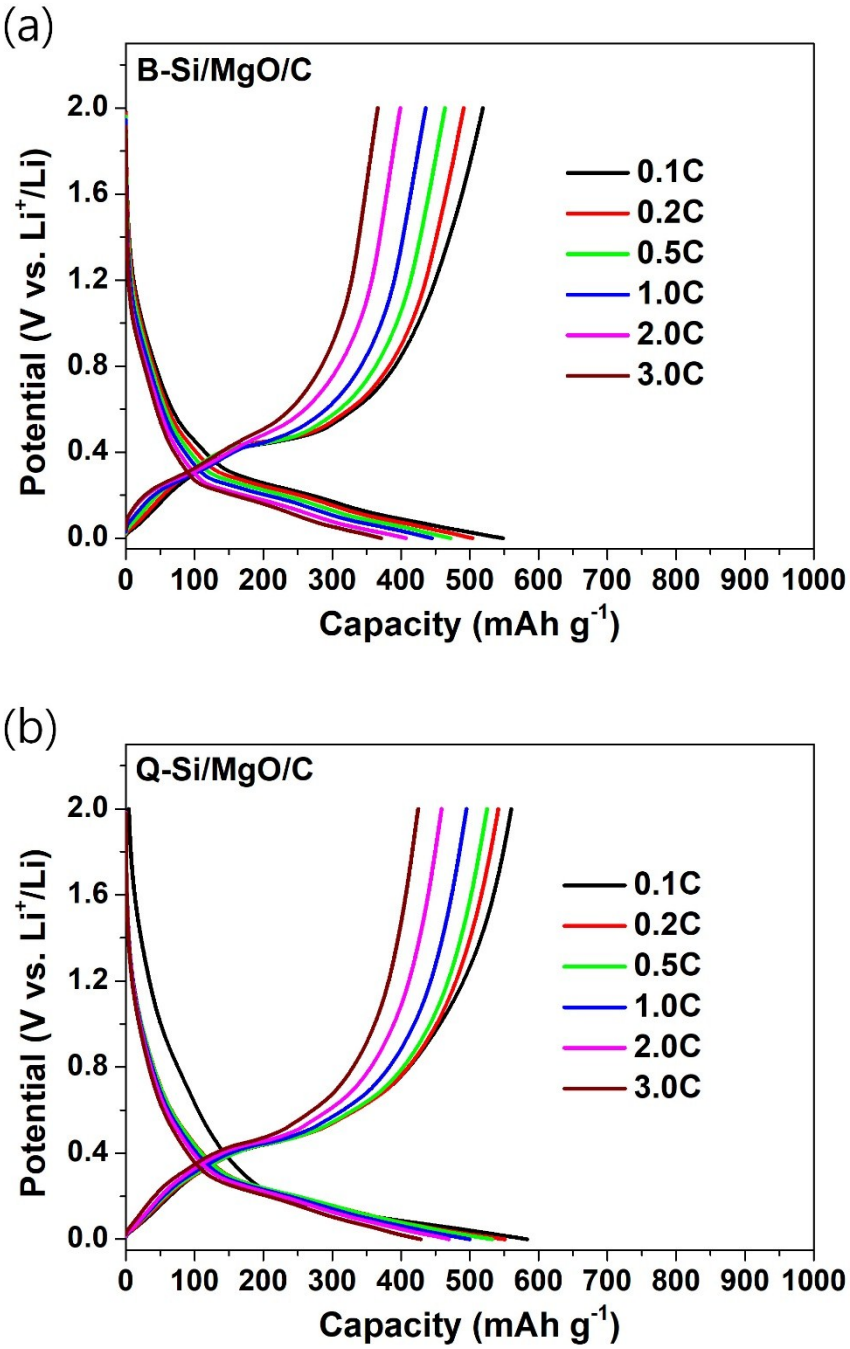

Figure S8. Voltage profiles at different C-rates of B-Si/MgO/C and Q-Si/MgO/C composite electrodes. (a) Voltage profiles of B-Si/MgO/C composite electrode. (b) Voltage profiles of Q-Si/MgO/C composite electrode.